Integration of Sub-6 GHz and mm-Wave Bands for 5G MIMO Smartphone Applications

Saiful Islam, Muhammad Zada, and Hyoungsuk Yoo*
Hanyang University, Seoul, Korea
saifulbd@hanyang.ac.kr, muhammadzada21@gmail.com, and *hsyoo@hanyang.ac.kr

I. INTRODUCTION

Modern mobile communication systems demand multi-band miniaturized antennas operating at lower GHz bands (sub-6 GHz), owing to the limited space in mobile phones [1]-[3]. Besides the limited space in mobile phones, the complex feeding techniques for multiple antennas may cause additional losses, particularly at the mm-wave bands that are more vulnerable to this issue; therefore, multiband antennas are the most preferred solution for 5G mobile applications. Presently, the realization of multiband antennas at sub-6 GHz and mm-wave bands has been the focus of research in this area.

II. METHODOLOGY

The geometry of the proposed 8 × 8 MIMO antenna is illustrated in Fig. 1. The eight designed antenna elements (Ant- 1-Ant-8), are placed along the two side-edges of the double-sided copper-cladding Rogers RT/duroid 5880 substrate, which has a dielectric permittivity (r) of 2.2, a loss tangent (tanδ) of 0.0009, and a thickness of 0.508 mm. The substrate dimensions are 157.7 mm × 70 mm, which are set similar to the dimensions of the Samsung galaxy S10 5G. The radiating patch (orange) and the ground plane (light blue) are printed on opposite sides of the substrate. The antennas orientated in a vertical position for the best utilization of space and to provide good isolation between the closest antenna elements; all the eight antennas are placed along the short edges, with four antennas on the topside (Ant-5–Ant- 8) and four on the bottom side (Ant-1–Ant-4). A 10-mm distance was kept between the two closest antenna elements to get the minimum isolation of 15 dB at a lower frequency. Initial antenna modeling, simulations, and optimization were conducted using the full-wave electromagnetic (EM), ANSYS high-frequency structure simulator (HFSS) software. Fig. 2(a) shows the current distribution at the sub-6-GHz (3.5 GHz) band with the inset views of a single-antenna element, including the radiating patch and the ground plane.

Acknowledgment:
This work was supported grant (2019R1A2C2004774).

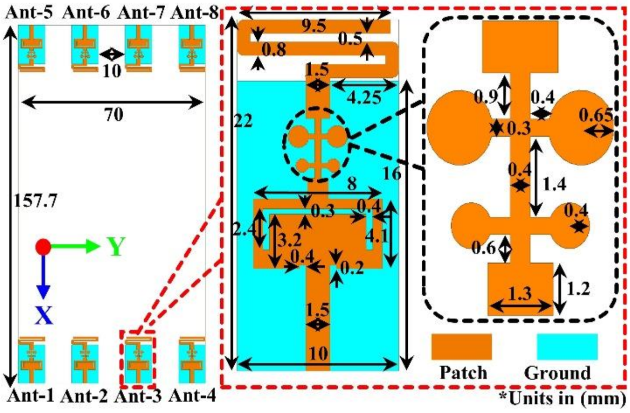

Fig. 1. Structure of the proposed MIMO antenna.

It can be observed that the magnitude of the current density is higher on the microstrip line and the current flowing toward the meandered shape antenna part via the CMRC LPF has a much higher current density over the meandered lines. As stated earlier, the filter works as a short circuit in the lower frequency applications and works as an open circuit in the higher frequency >20 GHz. Therefore, the surface currents pass through the filter from the lower part towards the upper meandered radiating structure. Similarly, Fig. 2(b) displays the surface current distribution on the radiating structures in mm-wave band of 28 GHz.

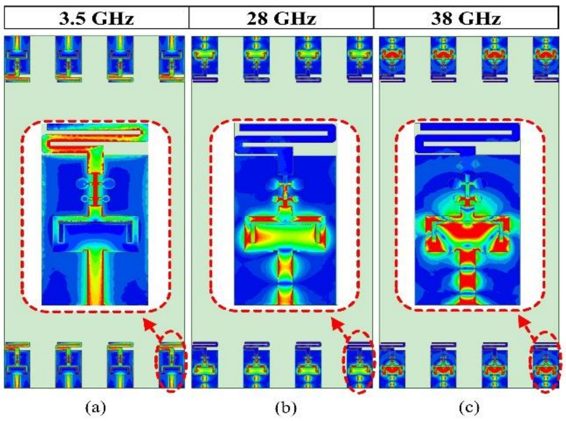

Fig. 2. Current (a) 3.5 GHz. (b) 28 GHz. (c) 38 GHz.

The surface currents mainly focused on the lower part of the antenna (the microstrip antenna loaded with a slot), In the microstrip patch part of the antenna, an inverted U-shape slot was introduced to generate the second resonance in the mm-wave band at 38 GHz and similar result observed.

III. RESULTS

Fig. 3 shows the simulated reflection coefficient (S22) and transmission coefficients (S23, S24, and S26) of the MIMO antennas across the desired frequency bands. Almost identical reflection coefficients were

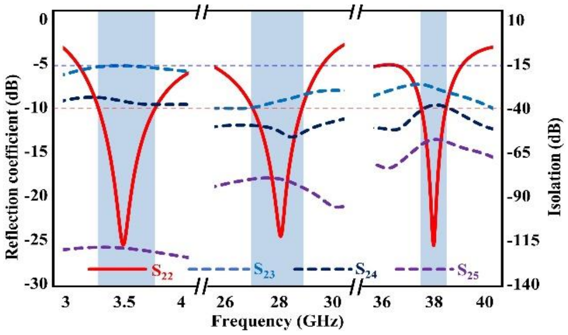

Fig. 3. Simulated scattering parameters.

observed because of the symmetrical placement of the identical antenna elements on the substrate; therefore, only the S22 (reflection coefficient of Ant-2) is plotted in Fig. 3. It can be observed that the proposed antenna

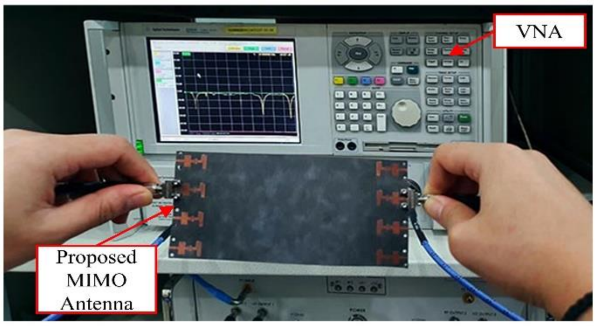

(a)

Fig. 4. Measurement setup for Scattering parameter.

are covering three useful bands of 3.5, 28, and 38 GHz with -10 dB bandwidths of 450 MHz (3.30–3.75 GHz), 1620 MHz (27.15–28.77 GHz), and 900 MHz (37.59–38.49 GHz), respectively. In Fig. 3 shows the isolation of >15 dB at the sub-6-GHz band was achieved between the nearest antenna elements (Ant-2 and Ant-3) while >35 and >120 dB isolation was observed between the Ant-2 to Ant-4 and Ant-2 to Ant-6, respectively. However, isolation at mm-wave was considerably improved, owing to the very short wavelength. In fig. 4 shows measurement setup of scattering parameter. Antenna efficiency and gain for was analyzed. Peak gains of 3.5, 8.2, and 8.7 dBi were attained and simulated efficiencies of 56%, 99%, and 99.5% for Ant-2 were realized. In fig. 5 comparison of measured and simulated radiation pattern (E-plane (XZ) and H-plane (YZ) has shown for all frequency.

IV. CONCLUSION

We discussed the integration of sub-6-GHz (3.5 GHz) and mm-wave bands (28 and 38 GHz) by using a CMRC

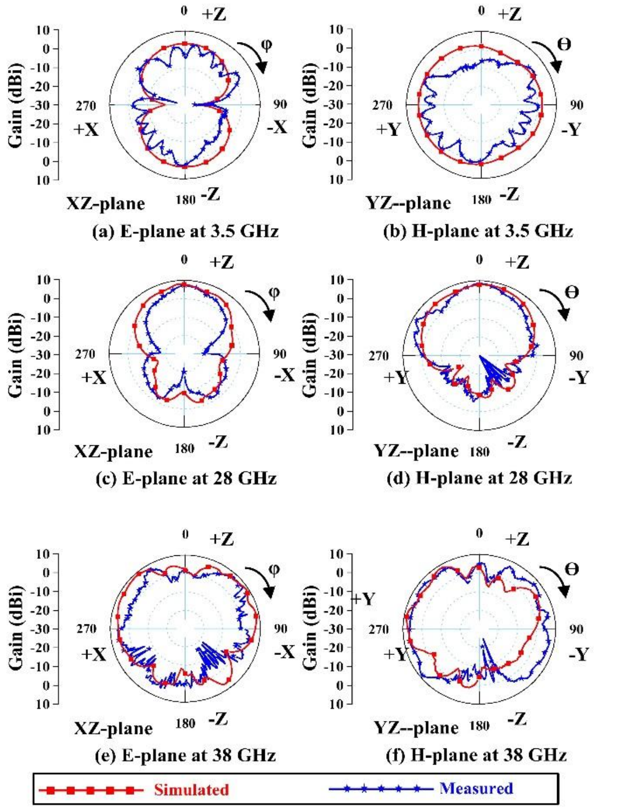

Fig. 5. Simulated and measurement radiation pattern.

LPF with a single-fed compact antenna for future 5G MIMO smartphone applications. The standalone size of the single antenna was kept small by using a meandered line backed by a truncated ground structure. Additionally, the MIMO performance was validated through a fabricated prototype of the proposed 8 × 8 MIMO antenna. Based on the diversity and radiation performance with a compact size, the proposed antenna can be a good addition to future 5G wireless communication.

V. REFERENCES

[1] Y. Liu, Y. Li, L. Ge, J. Wang, and B. Ai, “A compact hepta-band mode composite antenna for sub (6, 28, and 38) GHz applications,” IEEE Transactions on Antennas and Propagation, vol. 68, no. 4, pp. 2593–2602, 2020

[2] Y. Ban, Y. Qiang, Z. Chen, K. Kang, and J. Guo, “A dual-loop antenna design for hepta-band WWAN/LTE metal-rimmed smartphone applications,” IEEE Transactions on Antennas and Propagation, vol. 63, no. 1, pp. 48–58, 2015

[3] J.-W. Lian, Y.-L. Ban, Y.-L. Yang, L.-W. Zhang, K. Kang et al., “Hybrid multimode narrow-frame antenna for WWAN/LTE metal-rimmed smartphone applications,” IEEE Access, vol. 4, pp. 3991–3998, 2016